A Medical Image Classification Model based on Quantum-Inspired Genetic Algorithm

Hussain K. Ibrahim
National School of Electronics and Telecommunications (ENET'COM) of Sfax, University of Sfax, Tunisia | High Institute of Applied Science Technology of Sousse, University of Sousse, Tunisia | Research Groups in Intelligent Machines (REGIM Laboratory), National Engineering School of Sfax (ENIS), University of Sfax, Tunisia | College of Computer Science and Information Technology, Wasit University, Iraq
hussein.ibrahim.doc@enetcom.usf.tn (corresponding author)

Nizar Rokbani
High Institute of Applied Sciences and Technology of Sousse University of Sousse, Tunisia | Research Groups in Intelligent Machines (REGIM Laboratory), National Engineering School of Sfax (ENIS), University of Sfax, Tunisia | Department of Biomedical Technology, College of Applied Medical Sciences in Al-Kharj, Prince Sattam bin Abdulaziz University, Al-Kharj, 11942 Saudi Arabia
nizar.rokbani@ieee.org

Ali Wali
Higher Institute of Computer Science and Multimedia of Sfax, University of Sfax, Tunisia | Research Groups in Intelligent Machines (REGIM Laboratory), National Engineering School of Sfax (ENIS), University of Sfax, Tunisia
ali.wali@isims.usf.tn

Khmaies Ouahada
Department of Electrical and Electronic Engineering Science, University of Johannesburg, Auckland Park, South Africa
kouahada@uj.ac.za

Habib Chabchoub
College of Business, Al Ain University of Science and Technology, Abu Dhabi, United Arab Emirates
habib.chabchoub@aau.ac.ae

Adel M. Alimi
Research Groups in Intelligent Machines (REGIM Laboratory), National Engineering School of Sfax (ENIS), University of Sfax, Tunisia | Department of Electrical and Electronic Engineering Science, Faculty of Engineering and the Built Environment, University of Johannesburg, South Africa
adel.alimi@ieee.org

Received: 18 July 2024 | Revised: 1 August 2024 | Accepted: 4 August 2024

 DOI: https://doi.org/10.48084/etasr.8430

ABSTRACT

This study used a Quantum-Inspired Genetic Algorithm (QIGA) to select the proper functionality and reduce the dimensions, classification time, and computational cost of a learning dataset. QIGA reduces the complexity of solutions and improves the selection of the best features. The application of quantum principles, in particular the unpredictability of quantum chromosomes, which are represented by qubits, can help in investigating a significantly more extensive solution space. QIGA offers a novel approach to feature selection in optimization problems. Using principles from quantum computing, this algorithm aims to enhance the efficiency and effectiveness of the feature selection process to increase performance. This

indicates that features of both exploration and exploitation are embodied by QIGA without requiring massive amounts of data. Considerable gains in classification accuracy were achieved compared to traditional methods. The dynamic design of the models through the evolutionary mechanism in QIGA enables the optimization process to adapt to varying probabilities produced from the qubit overlay via the quantum rotation gate. This is contrary to traditional methods. The model using QIGA offered a more precise classification than the model optimized by Genetic Algorithms (GA). The proposed method achieved superior performance in terms of classification accuracy, with a score of more than 98%, compared to GA, which achieved a classification accuracy of 94%.

Keywords-medical image classification; deep learning; machine learning; genetic algorithm; quantum-inspired; K-nearest neighbors

I. INTRODUCTION

Approaches based on Machine Learning (ML) and Deep Learning (DL) have become increasingly popular in the field of healthcare for the diagnosis of a wide variety of diseases. The use of image processing has seen explosive growth in this sector, utilizing such methods in Medical Image Classification (MIC) [1]. Genetic Algorithms (GAs) are a class of evolutionary algorithms inspired by Darwinian natural selection. They are popular heuristic optimization methods based on simulated genetic mechanisms, i.e., mutation, crossover, etc., and population dynamical processes, such as reproduction, selection, etc. Solutions are encoded in arrays that are referred to as chromosomes. Usually, the algorithm begins with a randomly generated initial population of chromosomes and evolves over and over the population in search of an optimal solution. The drawback of these methods is that they require adequate data to train the model and increase prediction accuracy. This limitation is incompatible with the absence of accurate and adequate data in MIC [2, 3].

Quantum computing focuses on developing computer technology based on the principles of quantum theory. Quantum computers use quantum bits, or qubits, which process information very differently. While classical bits always represent either one or zero, Quantum Inspired Genetic Algorithms (QIGAs) offer a novel approach to feature selection in optimization problems, aiming to improve their efficiency and effectiveness. This study delves into the three key components of QIGA: qubit population representation, quantum rotation gate function, and crossover and mutation functions for quantum populations. By integrating the GA and the superposition principle, an effective improvement in MIC precision can be achieved. In addition, the results show that QIGA is much more efficient than Classic Genetic Algorithms (CGA). This development can be credited to the fact that QIGA can obtain a more exact classification by utilizing the superposition principle which is inherent in quantum computing. The incorporation of quantum concepts into evolutionary algorithms is a substantial advancement in the field of feature selection approaches. Quantum-inspired GAs have the potential to bring about a revolution in the field of healthcare diagnostics and contribute to improved patient outcomes and classification tasks in a variety of fields, including the treatment of medical conditions.

II. LITERATURE REVIEW

Many scholars tried to solve the aforementioned problems by developing the concept of information fusion, which has been very important in many fields. Based on the theory of text content, the technical definition of information fusion is the process of merging and associating information from one or multiple sources to produce meaningful information for detecting, identifying, and classifying a specific object [4]. Information fusion improves the accuracy of the predictions made by ML and DL models. Computed Tomography (CT) scans have been combined as a component of information fusion to be fed into DL models. Similar information fusion can be observed in works using chest X-ray images obtained from different repositories [4, 5]. In [6], different X-ray image datasets were combined and processed into a Convolutional Neural Network (CNN) for MIC [6]. In [7], Google Trends Data (GTD) was used in some countries, including Iran, China, Italy, and South Korea, to collect and fuse MIC information. However, these models could not distinguish between COVID-19 and other viral infectious diseases. Feature selection processes are deployed to increase performance and choose the significant features that affect the accuracy of model classification. Wrapper- and embedded-based feature selection methods have been used to choose the essential features. Then, the optimum number of features is extracted from the dataset, which includes various information and data types, suggesting a hybrid feature selection strategy: the filter method as a rapid feature selection and a GA to choose the important features extracted from chest CT images. Then, an Enhanced K-Nearest Neighbor (EKNN) classifier can be employed to detect COVID-19. In [8], an Adaptive Feature Selection-guided Deep Forest (AFS-DF) algorithm was applied to classify MIC using chest CT images, achieving an accuracy of 91.79%.

Various pre-trained CNNs have been implemented to identify MIC from X-ray images. The correlation-based feature selection technique, in combination with subset size forward selection and a linear forward selection-based search, have been used to select the best combination of features extracted from multi-CNNs. The Bayes classifier has achieved 91.16% accuracy when tested on a dataset with 453 COVID-19 images and 497 non-COVID images, and 97.44% on a dataset consisting of 71 COVID-19 images and 7 non-COVID images [9-11]. In [12], several ML algorithms were utilized to predict mortality in patients with COVID-19. A dataset with more than 117,000 laboratory-confirmed COVID-19 patients was used, achieving 93% accuracy. In [13, 14], two feature selection techniques were followed to select the optimal features that enhance the prediction, Recursive Feature Elimination (RFE) and Extra Tree Classifier (ETC), applying the Naive Bayesian (NB) and Restricted Boltzmann Machine (RBM) methods to classify feature vectors.

Traditional methods for choosing important features might lead to improved accuracy, but large amounts of data still depend on the optimization techniques used. To address this, in [15], a quantum optimization model was proposed for feature selection. Quantum computing concepts were combined with metaheuristic GAs to produce QIGA. Due to its fast convergence and powerful global search capabilities, QIGA can perform significantly better in a parallel structure, encompassing both exploration and exploitation features without the need for huge amounts of data.

This study aims to: (i) enhance conventional classification strategies by proposing a new QIGA for feature selection, and (ii) discuss the problems of computing cost and early convergence of traditional GA algorithms. By integrating the principles of quantum mechanics, particularly the superposition and entanglement properties of qubits, the proposed QIGA seeks to improve the efficiency and accuracy of feature selection in MIC. This approach not only demonstrates superior performance in terms of classification accuracy, but also reduces the required computational resources compared to classical methods. A series of trials show that the proposed QIGA technique is significantly more precise and faster than the alternatives [16]. The GA is an adaptive heuristic search algorithm used in medical image feature selection for classification. When it comes to dilemma complexity, in general, GA performs better than NN. Additionally, GA is resilient to selecting the optimal feature for the classification process, which causes the most visible problems. Optimizing the NN structure can attain both convergence and efficiency. There are numerous types of outcomes in NN design optimization. A GA can be utilized to create an artificial intelligence algorithm or "teaching", as the one used in [17-22].

III. SYSTEM OVERVIEW

Building on the strengths of GA, this section covers in detail the proposed QIGA that seeks to achieve a precise MIC for COVID-19, lung opacity, normal, and viral pneumonia. In the proposed system, quantum computing is deployed to harness the unpredictability provided by the probabilistic models of quantum chromosomes given by qubits to achieve variance in the population's assembly. This large diversity in each generation reduces the number of generations required for GA to find the optimal solution. QIGA offers a novel approach to feature selection in optimization problems. This study delves into the three key components of QIGA: qubit population representation, quantum rotation gate function, and crossover and mutation functions for quantum populations. Qubit population representation is a fundamental aspect of QIGA. In traditional GAs, the population of potential solutions is represented using binary strings or real-valued vectors. However, QIGA leverages the power of qubits, which are quantum bits capable of representing multiple states simultaneously. This unique property allows for parallel processing and exploration of multiple solutions at once. Instead of a single binary or real-valued representation for each solution, qubits enable the representation of multiple possible states simultaneously. For example, a qubit can represent both 0 and 1 at the same time, which is known as superposition. This feature allows QIGA to explore a larger search space and potentially discover more optimal subsets of features for the given problem. The second component of QIGA is the quantum rotation gate function. This function plays a crucial role in increasing the diversity of the population. In traditional GAs, diversity is typically achieved through mutation and crossover operations. However, in QIGA, the quantum rotation gate function introduces an additional mechanism for diversification. The quantum rotation gate function operates by rotating the qubit states in a controlled manner. This rotation alters the probability distribution of the qubit states, allowing for the exploration of different solution spaces. By manipulating the quantum states through rotations, QIGA can effectively explore a wider range of potential solutions and avoid getting trapped in local optima. Lastly, QIGA incorporates crossover and mutation functions specifically designed for quantum populations. These functions manipulate the qubit states to generate new solutions and introduce diversity to the population. Crossover involves combining the qubit states of two parent solutions to create offspring solutions. Mutation, on the other hand, introduces random changes to the qubit states. The crossover and mutation functions for the quantum population are tailored to take advantage of the unique properties of qubits. These functions ensure that the exploration of the solution space is not limited to classical genetic operators but also leverages the quantum properties of superposition and entanglement. This allows for a more effective search for optimal feature subsets.

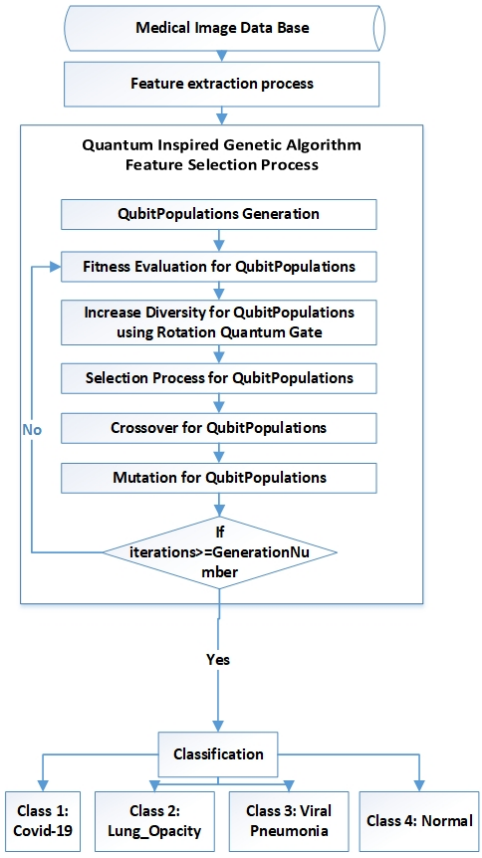

Fig. 1. QIGA feature selection process model.

QIGA offers a promising approach to feature selection in optimization problems. Qubit population representation, quantum rotation gate function, and crossover and mutation functions for quantum populations are key components that enhance the efficiency and effectiveness of the feature selection process. By leveraging these quantum-inspired techniques, QIGA can explore a larger search space, increase the diversity of the population, and potentially discover more optimal subsets of features. Figure 1 illustrates the proposed QIGA for feature selection for MIC.

The inspired quantum computing notion within GA leads to greater population variety than classical GA. Furthermore, the linear superposition of all conceivable binary states in quantum chromosomes allows significantly more variation than classical representation. A quantum rotation gate is used to converge the chromosomal individuals toward optimal solutions. Its primary goal is to test the modified QICA's MIC accuracy. The suggested strategy utilizes the notion of fitness superposition to improve the classic GA selection technique, minimize computation costs, and avoid early convergence. Furthermore, the specific notion is deployed to enhance variety while simultaneously controlling population selection in mutation (divergence) and cross-cutting (convergence) transactions.

A. QIGA for Feature Selection

The extracted features from the previous step are arranged from the first image in the matrix until the last image, and the feature vector includes the first features of each descriptor. In this work, the feature vector has a length of 184 and is fed to QIGA for feature selection. Generally, in QIGA, the qubit representation was adopted for minimization problems based on the concept and principles of quantum computing. The characteristic of the representation is that any linear superposition can be represented. The state of a qubit can be represented as follows: ∪ is an arbitrary single-qubit unitary operation, and Θ_i is the rotation angle for each qubit around the y-axis, defined as:

$$\Theta_i = S(\Theta_m, \beta_m) * \Delta\theta_i \quad (1)$$

where $S(\Theta_m, \beta_m)$ is the sign of θ_i that determines the direction and $\Delta\theta_i$ is the magnitude of the rotation gate. θ_i is required to provide the angle of rotation in radians, which can either be positive or negative. Θ_m^* and β_m^* are calculated as:

$$\begin{bmatrix}\Theta_m^* \\ \beta_m^*\end{bmatrix} = \cup(\theta)\begin{bmatrix}\Theta_m \\ \beta_m\end{bmatrix} \quad (2)$$

The first step of feature selection is initializing the population randomly and calculating the value of the population using the fitness function. The accuracy of classification is used as a fitness function. Then, the initial population is input into the quantum gate. A chromosome is logically equivalent to an m-qubit string of quantum vectors. All qubits can be tuned to the same value $1/\sqrt{2}$, which means that all basic quantum states are quantum superpositions with the same probability. The fitness function is also used to assess the new quantum population. For the result of a quantum population to be a decimal value, the state of each individual is converted from a decimal to a binary string before evaluation. The following method is deployed:

Create a random number τ in [0, 1]:

$$\tau|Z_{ij}^t|^2 \quad (3)$$

The assessing gen is set to be 1 else 0.

Then, save the weight set of the solution with its fitness. The finest tree and its fitness, along with its binary solution $P(t)$ are formerly nominated and deposited for following generations. The renewal policy is to match the fitness $f(x_i)$ of the recently quantified rate of the item with the current evolutionary goal's fitness $f(b_i)$. If $f(x_i) > f(b_i)$, then fine-tune the qubit of the related bit $f(x_i) /= f(b_i)$ to force the likelihood value to progress near the track of promoting the appearance of x_i. In contrast, if $f(x_i) < f(b_i)$, regulate the qubit of the equivalent bit to attain the likelihood scale and go forward in the track of aiding the presence of b_i. Adittionally, δ is the updating's angle step. The value of δ influences the speed of the convergence: If the value is large, the resolution may move away or have an early convergence to a local optimum. In this, the dynamic tuning of δ is approved, so that, it receives a value between 0.2π and 0.8π by dynamic tuning as stated by the variance of the genetic generations.

B. Architecture of Feature Extraction

The literature identifies four basic categories of characteristics: statistical, structural, model-based, and automated [23, 24]. Statistical characteristics are mathematical and statistical measurements used to classify relevant data and narrow the gap between classes. They have both global and local characteristics. Global characteristics describe the image's global characteristics. In local feature extraction, medical images are divided into several units or segments, and features are retrieved from a particular section of the image [23], which share a common description.

At each pixel position, the canonical LBP operator is generated by computing the values of a small circular neighborhood (with radius *R* pixels) surrounding the value of a center pixel. The key interest attribute is a common method for identifying points of interest, often known as important points. The image is then represented by a suitable descriptor of these identifying characteristics, such as Speed Up Robust Feature (SURF) [24], which is a quick and reliable approach to the local, similarity-invariant encoding and comparison of pictures. Real-time applications, such as object recognition and tracking, are made possible by the SURF technique's emphasis on the rapid calculation of operators. It consists of two steps: feature description and feature extraction. This study uses three types of statistical features: local features LPB, SURF, and global features from accelerated segment tests [25]. The FAST algorithm detects the edge pixels of the input image. If several pixels around a particular pixel are either brighter or darker than it, it is considered an image edge. The FAST approach determines the pixels around a center candidate pixel p to be those that occur on a Bradenham circle with radius R and created by the function B. These pixels are called candidates $B(R, p)$.

In the domain of verification, multiple types of features are utilized to enhance the performance of the model. There are numerous medical image formats. Some of them are lengthy,

whereas others are brief, and some are graphic whereas others are scripted. Some medical images contain lengthy vertical or horizontal strokes, while others are distorted, angled, etc. Moreover, medical image styles vary based on scripts. Thus, the same elements are not effective for all medical image styles. The stability of the features influences the identification rate and the style of the medical images also affects the recognition rate.

The main ability of quantum computing is to address unique challenges that would require a powerful traditional machine. Because micro- and macro-space searches are merged into many different genetic operators, genetic-inspired quantum computers are used in broad search areas while maintaining the link between efficiency and success. In classic quantum-inspired scanning processes, the definition of a superposition state is employed to solve combinational issues that modify the individual variables. The tendency of a quantum gadget to reside in many locations (states) at the same time is called overlapping. The precise superposition of states is the true power in quantum computation. Traditional computers are always in the same state. Quantum computers can exist in a state of superposition. This is the final parallel processing.

In QIGA, a single qubit is employed to keep and represent one gene. Each qubit may be in the 1 state, the 0 state, or any superposition of the two. The data expressed by this gene are not stable but still probable. Thus, when a process is passed on this gene, it can finish with all possible information simultaneously. Here, each gene has one qubit. The straightforward resolution is to approve the binary coding procedure in GA to code these qubits of multi-states. This technique has superior flexibility and is simpler to understand, as one qubit is used to represent one gene. Each qubit may reside in the superposition of the two quantum states concurrently. In general, multi-qubits are utilized to embody the multi-state operator node as follows:

$$q_j^t = \begin{bmatrix} Z_1^t & Z_2^t & \cdots & Z_m^t \\ \beta_1^t & \beta_2^t & \cdots & \beta_m^t \end{bmatrix} \quad (4)$$

q_j^t represents the chromosome of the t-th generation and the j-th individual, and m is the gen index number. Employing qubit encoding allows one to embody the superposition of multiple states instantaneously, forcing the QIGA to be better in terms of diversity compared to the classic GA algorithm. As stated in [1], convergence can also be achieved with the qubit statement. As Z_2 or β_2 attitudes to 0 or l, the qubit chromosome joins one single state. For the updating implementation procedure, a quantum rotation gate is used, as described by:

$$\cup(\theta_i) = \begin{bmatrix} cos\,\theta_i & -sin\,\theta_i \\ sin\,\theta_i & cos\,\theta_i \end{bmatrix} \quad (5)$$

The intensity of the pixel in the center of the circle is indicated by I_p, while the intensity of the surrounding pixels is represented by $I_p \to x$. There are three possible states of pixels on the circle: brighter, darker, or similar. $S_p \to x$ is the status of a pixel on the circle. FAST is used to determine if at least N sequential pixels in the circle, named arc, have the same, brighter, or darker state than the candidate pixel (plus or minus a threshold t). The equations below show a concise summary of these concepts:

$$\Sigma\pi \to \xi = \begin{cases} brighter, & I_p + t \geq I_p \to x \\ darker, & I_p \to x \geq I_p + t \\ similar, & I_p - t < I_p \to x < I_p + t \end{cases} \quad (6)$$

$$I_p \to x = B(R,p) \quad (7)$$

The extracted features are arranged from the first image in the matrix until the last image and the feature vector include the first features of each descriptor. In this study, the feature vector has a length of 184.

```
Algorithm 1: Q-coded GA
Input: Dataset T, No. of Generation t, No. of
individual's j, Initial Populations Pops
1:  QubitPops ←
      GenerateQuantumPopulation(Decimal_Features)
2:  while t < MAX_GENS do
3:    t ← t+1
4:    Fitness_Vals = Fitness_Evaluation(QubitPops)
5:    QubitPop← Selection_Best(QubitPops,
        Fitness_Vals)
6:    Update QubitPops using Q-gate
7:    If Termination_Condition is False, then
8:      for i ← 0 to (QubitPops _SIZE - 1) do
9:        New_QubitPops(i) ← Crossover(QubitPops)
10:       New_QubitPops(i) ←
            Mutation(New_QubitPops)
11:     end
12:     QubitPops = New_QubitPops
13:   end
14:   If Termination_Condition is True, then
15:     Return QubitPops
16:   end
17: end
18: Best_individual= QubitPop
```

C. Classification

The KNN algorithm is a non-parametric supervised learning approach. It utilizes the inputs of *k* training samples in a dataset that are the most similar to each other. The output is a class object that has been classified by a majority vote of its neighbors, with the object being assigned to the class that is the most frequent among its *k* closest neighbors. If *k* equals *n*, the item is automatically placed in the class corresponding to its *n* closest neighbors. The distance between the query features and the training features is determined by Euclidean distance as:

$$dis(x,y) = \sqrt{\sum_{i=1}^{n}(x_i - y_i)^2} \quad (8)$$

where *n* refers to data size.

IV. SIMULATION AND RESULTS

The proposed system scored the highest classification accuracy of over 98% in this evaluation utilizing conventional benchmarks. This result demonstrates improved MIC accuracy compared to the GA algorithm, which achieved 94%, as depicted in Tables II and III

A. Experimental Protocol and Dataset Description

The dataset used in this study includes four types (COVID-19, lung opacity, normal, and viral pneumonia) and 21,165 pictures. Figure 2 portrays some example images.

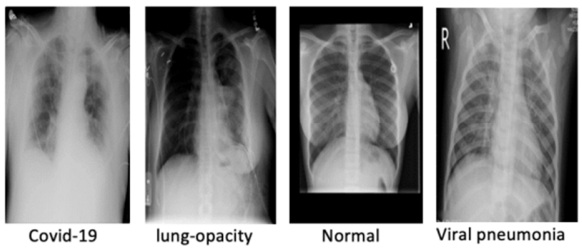

Fig. 2. Dataset sample.

B. Results

Two experiments were conducted deploying GA and QIGA. Classification accuracy was used as a fitness function. The data were randomly divided into 80% for training and 20% for testing. In the first experiment, classic GA was utilized to select the optimal features. Table I exhibits the GA parameters and Table II displays its results. In the second experiment, QIGA was used for feature selection. Table III shows the QIGA parameters and Table IV demonstrates its results.

TABLE I. GA PARAMETERS

Parameter	Default value
Population size	20
Generation number	20
Crossover ratio	0.7
Mutation ratio	0.3
Test ratio	022

TABLE II. RESULTS OF CLASSIC GA

Descriptor			Accuracy	Times	Confusion matrix
SURF	LPB	FAST			
√	√		94.70	168.405	Figure 3
√		√	94.16	92.444	Figure 4
	√	√	94.73	138.463	Figure 5

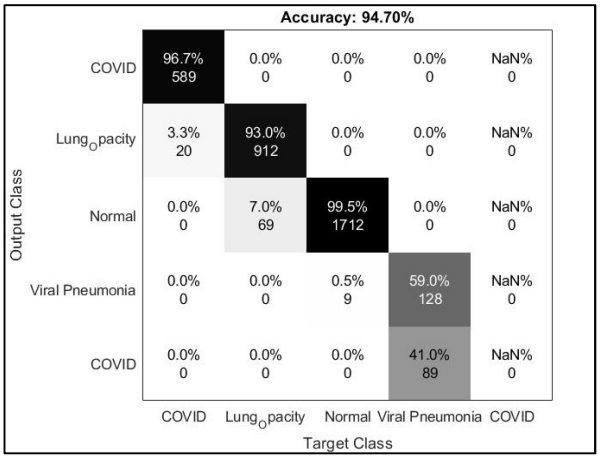

Fig. 3. Experimental versus classified modulation using GA.

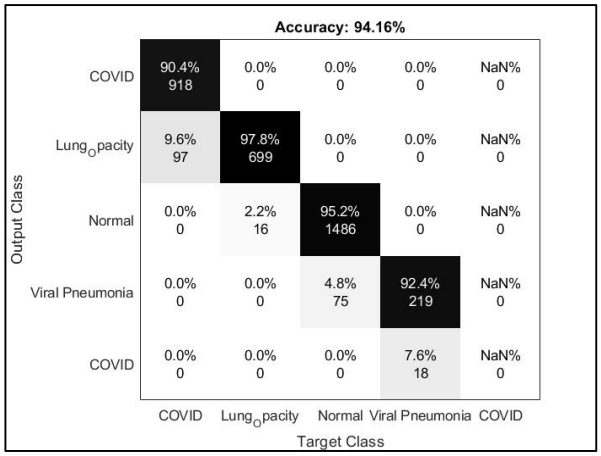

Fig. 4. Experimental versus classified modulation using GA.

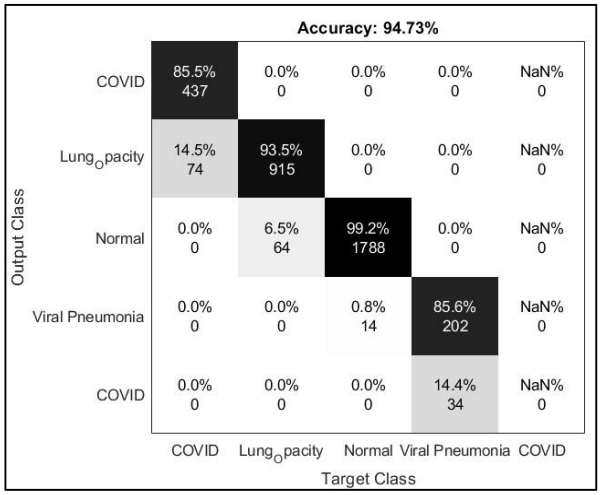

Fig. 5. Experimental versus classified modulation using the GA.

TABLE III. PARAMETERS OF QIGA

Parameter	Default value
Population size	5
Generation number	5
Crossover ratio	0.7
Mutation ratio	0.3
Test ratio	0.2

TABLE IV. RESULTS OF QIGA

Descriptor			Accuracy	Times	Confusion matrix
SURF	LPB	FAST			
√	√		98.36	75.306	Figure 6
√		√	98.81	32.279	Figure 7
	√	√	97.76	63.751	Figure 8

As evidenced in Tables II and IV, in each trial, two types of features were combined to test the ability of the selection processes for GA and QIGA based on KNN accuracy. According to the results, the superiority of the QIGA method is readily observed.

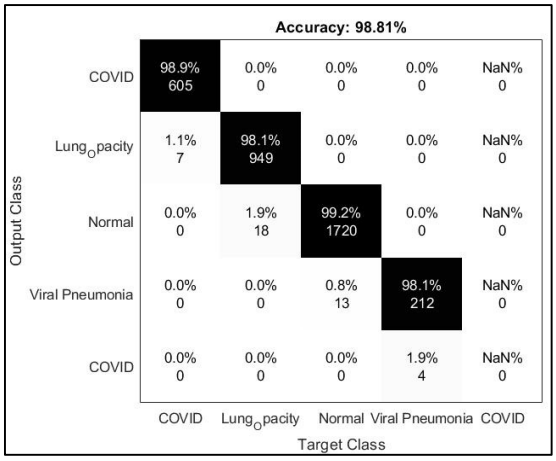

Fig. 6. Experimental versus classified modulation using QIGA.

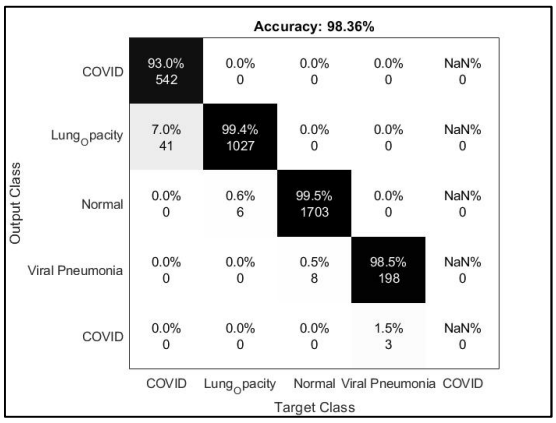

Fig. 7. Experimental versus classified modulation using QIGA.

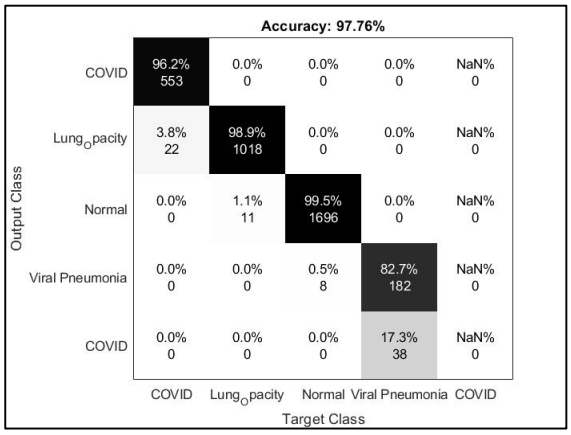

Fig. 8. Experimental versus classified modulation using QIGA.

QIGA was also evaluated in comparison to the GA based on F-score, population size, best fitness, average fitness, worst fitness, false reject rate, and false accept rate, as illustrated in Table V. For traditional GA, the sample size was 30, and the mean score was 94.1980 with a standard deviation of 1.65501. The minimum score observed was 90.06, and the maximum score was 97.19. For the QIGA, the sample size was 30, and the mean score was 97.2763 with a standard deviation of 0.78118. The minimum score observed was 95.83 and the maximum was 98.72. These descriptive statistics provide a summary of the performance of both algorithms. The QIGA algorithm shows a higher mean score and lower standard deviation compared to GA, indicating that it performs better on average and has less variability in its results. The minimum and maximum scores also suggest that QIGA outperforms GA in terms of finding more optimal solutions.

TABLE V. COMPARISON BETWEEN GA AND QIGA

Criteria	GA	QIGA
Population size	20	5
Best fitness	94.73	98.81
Worst fitness	92.4	94.5
F score	0.9470	0.9881
Time	138.463	32.279
False reject rate	9.5	1.43
False accept rate	5.54	0.95

Table VI shows the Wilcoxon signed ranks test results, which is a non-parametric statistical test used to determine if there is a significant difference between two related samples. This test is used to compare the performance of QIGA and GA. The ranks Table shows the number of negative ranks, where QIGA had a lower score than GA, and positive ranks, where QIGA had a higher score than GA. In this case, there was one negative rank and 29 positive ranks. Based on these results, it can be concluded that QIGA performs significantly better than GA, as indicated by the higher number of positive ranks and the higher mean rank for the positive ranks. Table VII illustrates the statistical value calculated (Z = -4.741), indicating the rejection of the null hypothesis and the acceptance of the alternative hypothesis.

TABLE VI. WILCOXON SIGNED RANKS TEST

Ranks				
		N	Mean rank	Sum of ranks
QIGA - GA	Negative Ranks	1[a]	2.00	2.00
	Positive Ranks	29[b]	15.97	463.00
	Ties	0[c]		
	Total	30		

a. QIGA < GA, b. QIGA > GA, c. QIGA = GA

TABLE VII. STATISTICAL VALUE

Test Statistics	
	QIGA – GA
Z	-4.741-[b]
Asymp. Sig. (2-tailed)	.000

b. Based on negative ranks.

TABLE VIII. WILCOXON SIGNED RANKS TEST

Ranks				
		N	Mean rank	Sum ranks
QIGA - GA	Negative ranks	30[a]	15.50	465.00
	Positive ranks	0[b]	.00	.00
	Ties	0[c]		
	Total	30		

a. QIGA < GA, b. QIGA > GA, c. QIGA = GA

In Table VIII, the Wilcoxon test values are calculated for three cases, namely (a) QIGA < GA, which demonstrated that

all values are less, i.e., time is less, and (b) QIGA > GA. There were no equal values for (c) QIGA = GA. As shown in Table IX, the median for the values of GA is 172.8521, for QIGA is 76.2247567, and the calculation of the upper and lower limits displays a standard deviation of 8.40960 for GA, which is greater than that of QIGA (0.69288279).

TABLE IX. TIME COMPARISON

Descriptive Statistics					
	N	**Mean**	**Std. deviation**	**Minimum**	**Maximum**
GA	30	172.8521	8.40960	154.81	192.07
QIGA	30	76.2247567	.69288279	74.94100	77.54800

V. COMPARATIVE ANALYSIS

Based on the experimental results, the accuracy of the classification and the ratio of true classification to false classification for COVID-19, lung opacity, and viral pneumonia, were improved when SURF was combined with FAST and the GN and PS of GA were set to 20. However, the computation time was increased. On the other hand, the best classification results were obtained when using QIGA with five generations and less computation time. The simulation findings demonstrate the potential of the proposed technique to obtain a detailed classification of COVID-19. The proposed system scored the highest classification accuracy of 98.81% utilizing conventional benchmarks. Compared to standard classification algorithms, GA was capable of successfully modeling composite real-world relations. Despite the improvements in classification accuracy achieved by GA, the results disclose that GA can choose features well with a large dataset. However, QIGA leads to greater population variety than classic GA. This variety helps to obtain optimal solutions with the best fitness functions, which can then be used to select the best linear equation. Moreover, a framework was designed using CNN to diagnose COVID-19 patients using chest X-ray images. A pre-trained Google Net was put into service, implementing transfer learning. A 20-fold cross-validation was considered to avoid overfitting. Finally, multi-objective GA was considered to tune the hyperparameters of the proposed COVID-19 identification in chest X-ray images. Although the model showed improved results when the number of epochs increased, after 300 epochs, no improvement was observed.

It is often beneficial to experiment with different algorithms and evaluate their performance on a particular task. Generally, during ten trials with the simulation setup configuration of multiple generations equal to 100, crossover probability at 0.8, and mutation probability of 0.2, the findings reveal that the QIGA with five individuals can surpass the GA with 20 individuals in terms of both best and mean fitness. Furthermore, the test results demonstrate a statistically significant differentiation between GA and QIGA. The statistical analysis results in Tables V and IX show the significance of QIGA in terms of accuracy and complexity. The proposed QIGA method scored the highest classification accuracy of more than 98% in this evaluation utilizing conventional benchmarks compared to the GA algorithm, which achieved 94%.

TABLE X. COMPARATIVE DISCUSSION OF THE PROPOSED WITH COMPETENT METHODS

Reference	**Dataset**	**Approach and techniques**	**Accuracy**
[26]	CHEST X-RAY scans	CNN and HOG	95.36%
[27]	392 CHEST X-rays (50% positive, 50% negative	Pre-processing CNN, Adam optimizer with learning rate 0.001.	94.44%
[28]	COVID-19 datasets	CNN with Keras Image Generator	94.56%
[29]	ImageNet dataset	Deep learning pipeline model	95%
[30]	x-ray	Particle swarm optimization PSO + Neural Network (NN)	96%
[31]	x-ray	ResNet feature extraction networks to construct the ResUNet++ network	96.36%
[32]	x-ray	CNN	97%
Proposed method	x-ray	QIGA Feature Selection Process	98.81

VI. CONCLUSION AND FUTURE WORKS

This study presented a groundbreaking method for selecting features using limited data samples. By integrating the GA and the superposition principle, and utilizing the capabilities of KNN and DL in the field of MIC, the study achieved considerable gains in classification accuracy in less time compared to traditional methods. The application of quantum principles, in particular the unpredictability of quantum chromosomes represented by qubits, has made it possible to investigate a solution space that is significantly more extensive. The dynamic design of models through the evolutionary mechanism in QIGA enables the optimization process to adapt to varying probabilities produced from the qubit overlay via the quantum rotation gate. This is in contrast to traditional methods. The results demonstrated that QIGA was better in terms of classification accuracy and required less computation time compared to previous models optimized by GA. Evaluation of the QIGA model using four types of medical images, including COVID-19, lung opacity, normal, and viral pneumonia cases, produced encouraging findings. Future research endeavors should focus on scalability and generalization. It would be extremely important to investigate the scalability of QIGA to handle larger datasets as well as its generalization to different classifications. When applied to real-world circumstances, having a solid understanding of the strengths and limitations of QIGA can provide extremely helpful insights into its applicability.

REFERENCES

[1] Q. Zhang, L. T. Yang, Z. Chen, and P. Li, "A survey on deep learning for big data," *Information Fusion*, vol. 42, pp. 146–157, Jul. 2018, https://doi.org/10.1016/j.inffus.2017.10.006.

[2] R. A. Hasan, M. F. Alomari, and J. B. Jamaluddin, "Comparative study: Using machine learning techniques about rainfall prediction," *AIP Conference Proceedings*, vol. 2787, no. 1, Jul. 2023, Art. no. 050014, https://doi.org/10.1063/5.0148472.

[3] F. Alam Khan, M. Asif, A. Ahmad, M. Alharbi, and H. Aljuaid, "Blockchain technology, improvement suggestions, security challenges on smart grid and its application in healthcare for sustainable development," *Sustainable Cities and Society*, vol. 55, Apr. 2020, Art. no. 102018, https://doi.org/10.1016/j.scs.2020.102018.

[4] F. Alam Khan, M. Asif, A. Ahmad, M. Alharbi, and H. Aljuaid, "Blockchain technology, improvement suggestions, security challenges on smart grid and its application in healthcare for sustainable development," *Sustainable Cities and Society*, vol. 55, Apr. 2020, Art. no. 102018, https://doi.org/10.1016/j.scs.2020.102018.

[5] A. Aboud *et al.*, "A Distributed Multifactorial Particle Swarm Optimization Approach." TechRxiv, https://doi.org//10.36227/techrxiv. 17260040.v1.

[6] I. D. Apostolopoulos and T. A. Mpesiana, "Covid-19: automatic detection from X-ray images utilizing transfer learning with convolutional neural networks," *Physical and Engineering Sciences in Medicine*, vol. 43, no. 2, pp. 635–640, Jun. 2020, https://doi.org/ 10.1007/s13246-020-00865-4.

[7] S. M. Ayyoubzadeh, S. M. Ayyoubzadeh, H. Zahedi, M. Ahmadi, and S. R. N. Kalhori, "Predicting COVID-19 Incidence Through Analysis of Google Trends Data in Iran: Data Mining and Deep Learning Pilot Study," *JMIR Public Health and Surveillance*, vol. 6, no. 2, Apr. 2020, Art. no. e18828, https://doi.org/10.2196/18828.

[8] L. Sun *et al.*, "Adaptive Feature Selection Guided Deep Forest for COVID-19 Classification With Chest CT," *IEEE Journal of Biomedical and Health Informatics*, vol. 24, no. 10, pp. 2798–2805, Jul. 2020, https://doi.org/10.1109/JBHI.2020.3019505.

[9] Z. Laboudi and S. Chikhi, "Comparison of Genetic Algorithm and Quantum Genetic Algorithm," *The International Arab Journal of Information Technology*, vol. 9, no. 3, pp. 243–249, 2012.

[10] R. H. Ali and W. H. Abdulsalam, "The Prediction of COVID 19 Disease Using Feature Selection Techniques," *Journal of Physics: Conference Series*, vol. 1879, no. 2, Feb. 2021, Art. no. 022083, https://doi.org/ 10.1088/1742-6596/1879/2/022083.

[11] A. Aboud, N. Rokbani, S. Mirjalili, A. Hussain, H. Chabchoub, and A. M. Alimi, "A Quantum Beta Distributed Multi-Objective Particle Swarm Optimization Algorithm for Twitter Fake Accounts Detection." TechRxiv, Jul. 14, 2023, https://doi.org/10.36227/techrxiv.19461080.v2.

[12] Y. Soussi, N. Rokbani, M. M. B. Khelifa, A. Wali, and N. T. Phuong, "Clustering multi-objectifs basée sur l'algorithme d'essaim de salpedia bêta- distribués (Multi-Objectif Beta Salp Swarm Algorithm MO-β-SSA)," Laboratoire LIS, Carqueiranne, France, May 2023.

[13] C. Mair *et al.*, "An investigation of machine learning based prediction systems," *Journal of Systems and Software*, vol. 53, no. 1, pp. 23–29, Jul. 2000, https://doi.org/10.1016/S0164-1212(00)00005-4.

[14] A. A. Abdulhussien, M. F. Nasrudin, S. M. Darwish, and Z. Abdi Alkareem Alyasseri, "Feature selection method based on quantum inspired genetic algorithm for Arabic signature verification," *Journal of King Saud University - Computer and Information Sciences*, vol. 35, no. 3, pp. 141–156, Mar. 2023, https://doi.org/10.1016/j.jksuci.2023.02.005.

[15] N. Zeng, Z. Wang, W. Liu, H. Zhang, K. Hone, and X. Liu, "A Dynamic Neighborhood-Based Switching Particle Swarm Optimization Algorithm," *IEEE Transactions on Cybernetics*, vol. 52, no. 9, pp. 9290–9301, Sep. 2022, https://doi.org/10.1109/TCYB.2020.3029748.

[16] A. R. Lubis, M. Lubis, and A. Khowarizmi, "Optimization of distance formula in K-Nearest Neighbor method," *Bulletin of Electrical Engineering and Informatics*, vol. 9, no. 1, pp. 326–338, Feb. 2020, https://doi.org/10.11591/eei.v9i1.1464.

[17] A. A. Abdulhussien, M. F. Nasrudin, S. M. Darwish, and Z. Abdi Alkareem Alyasseri, "Feature selection method based on quantum inspired genetic algorithm for Arabic signature verification," *Journal of King Saud University - Computer and Information Sciences*, vol. 35, no. 3, pp. 141–156, Mar. 2023, https://doi.org/10.1016/j.jksuci.2023.02.005.

[18] S. M. Darwish, I. A. Mhaimeed, and A. A. Elzoghabi, "A Quantum Genetic Algorithm for Building a Semantic Textual Similarity Estimation Framework for Plagiarism Detection Applications," *Entropy*, vol. 25, no. 9, Sep. 2023, Art. no. 1271, https://doi.org/10.3390/ e25091271.

[19] M. Khanna, A. Agarwal, L. K. Singh, S. Thawkar, A. Khanna, and D. Gupta, "Radiologist-Level Two Novel and Robust Automated Computer-Aided Prediction Models for Early Detection of COVID-19 Infection from Chest X-ray Images," *Arabian Journal for Science and Engineering*, vol. 48, no. 8, pp. 11051–11083, Aug. 2023, https://doi.org/10.1007/s13369-021-05880-5.

[20] T. T. Nguyen, N. Q. Luc, and T. T. Dao, "Developing Secure Messaging Software using Post-Quantum Cryptography," *Engineering, Technology & Applied Science Research*, vol. 13, no. 6, pp. 12440–12445, Dec. 2023, https://doi.org/10.48084/etasr.6549.

[21] A. H. Alaidi, C. S. Der, and Y. W. Leong, "Increased Efficiency of the Artificial Bee Colony Algorithm Using the Pheromone Technique," *Engineering, Technology & Applied Science Research*, vol. 12, no. 6, pp. 9732–9736, Dec. 2022, https://doi.org/10.48084/etasr.5305.

[22] A. H. Alaidi, S. D. Chen, and Y. W. Leong, "Artificial Bee Colony with Crossover Operations for Discrete Problems," *Engineering, Technology & Applied Science Research*, vol. 12, no. 6, pp. 9510–9514, Dec. 2022, https://doi.org/10.48084/etasr.5250.

[23] H. Zhang, H. Xu, X. Tian, J. Jiang, and J. Ma, "Image fusion meets deep learning: A survey and perspective," *Information Fusion*, vol. 76, pp. 323–336, Dec. 2021, https://doi.org/10.1016/j.inffus.2021.06.008.

[24] K. T. Powers and J. D. Santoro, "Metabolic stroke-like episode in a child with FARS2 mutation and SARS-CoV-2 positive cerebrospinal fluid," *Molecular Genetics and Metabolism Reports*, vol. 27, Jun. 2021, Art. no. 100756, https://doi.org/10.1016/j.ymgmr.2021.100756.

[25] T. Tuncer, "Fusion and Deep Learning," *Computers, Materials & Continua*, vol. 64, 2021, Art. no. 102257.

[26] T. Rahman, M. Chowdhury, and A. Khandakar, "COVID-19 Radiography Database." [Online]. Available: https://www.kaggle.com/ datasets/tawsifurrahman/covid19-radiography-database.

[27] V. Madaan *et al.*, "XCOVNet: Chest X-ray Image Classification for COVID-19 Early Detection Using Convolutional Neural Networks," *New Generation Computing*, vol. 39, no. 3, pp. 583–597, Nov. 2021, https://doi.org/10.1007/s00354-021-00121-7.

[28] M. Umer, I. Ashraf, S. Ullah, A. Mehmood, and G. S. Choi, "COVINet: a convolutional neural network approach for predicting COVID-19 from chest X-ray images," *Journal of Ambient Intelligence and Humanized Computing*, vol. 13, no. 1, pp. 535–547, Jan. 2022, https://doi.org/ 10.1007/s12652-021-02917-3.

[29] S. Albahli and G. N. A. H. Yar, "Fast and Accurate Detection of COVID-19 Along With 14 Other Chest Pathologies Using a Multi-Level Classification: Algorithm Development and Validation Study," *Journal of Medical Internet Research*, vol. 23, no. 2, Feb. 2021, Art. no. e23693, https://doi.org/10.2196/23693.

[30] H. K. Ibrahim, N. Rokbani, A. Wali, and A. M. Alimi, "GA-NN and PSO-NN for Medical Images Classification: A Comparative Analysis," in *2023 IEEE International Conference on Artificial Intelligence & Green Energy (ICAIGE)*, Sousse, Tunisia, Oct. 2023, pp. 1–6, https://doi.org/10.1109/ICAIGE58321.2023.10346503.

[31] M. Chavan, V. Varadarajan, S. Gite, and K. Kotecha, "Deep Neural Network for Lung Image Segmentation on Chest X-ray," *Technologies*, vol. 10, no. 5, Oct. 2022, Art. no. 105, https://doi.org/10.3390/ technologies10050105.

[32] S. Mathesul *et al.*, "COVID-19 Detection from Chest X-ray Images Based on Deep Learning Techniques," *Algorithms*, vol. 16, no. 10, Oct. 2023, Art. no. 494, https://doi.org/10.3390/a16100494.